Zintl Phases in Alkali-Metal−Tin Systems: K_8Sn_{25} with Condensed Pentagonal Dodecahedra of Tin. Two A_8Sn_{44} Phases with a Defect Clathrate Structure

Jing-Tai Zhao and John D. Corbett*

Ames Laboratory[1] and Department of Chemistry, Iowa State University, Ames, Iowa 50011

Received April 21, 1994[⊗]

Single-phase K_8Sn_{25} is synthesized from the elements on annealing below 400 °C. The phase is somewhat nonstoichiometric, and the lattice constant also depends on thermal history. The structure was solved for $K_{7.4(1)}Sn_{25}$ (s.g. $P4_132$, $Z = 4$, $a = 16.294(5)$ Å, $R/R_w = 4.0/3.6\%$ for 833 observed reflections and 55 parameters). The new structure type contains pentagonal dodecahedra of tin that share three pentagonal faces with like members and are also interconnected to another cage through a single exo bond. Tin−tin distances are very similar to those in gray tin and in Rb_8Sn_{44}. The three types of potassium ions are (1) encapsulated in each Sn_{20} cage, (2) bonded in tin octahedra between clusters, and (3) somewhat disordered in channels through the tin network. Eight tin atoms per formula unit are three-bonded, the remainder four-bonded, and the ideal compositon $K_{8.0}Sn_{25}$ is, appropriately, a diamagnetic semiconductor. An analogous compound does not form in the binary rubidium or cesium systems. The crystal structures of the isostructural $Rb_8Sn_{44.6(1)}$ and $K_{1.6(2)}Cs_{6.4(2)}Sn_{44.0(1)}$ were also refined ($Pm\bar{3}n$, $Z = 1$, $a = 12.054(1)$, 12.084(1) Å, $R/R_w = 7.6/6.7$, 6.6/5.7, respectively). These are defect members of the clathrate-I $A_8(H_2O)_{46}$ type structure with one-third random vacancies at the 6*c* positions and classical Zintl phases. K_8Sn_{44} was shown to be a diamagnetic semiconductor.

Introduction

Seven phases are reported in the current K−Sn phase diagram, which dates largely to 1908.[2] Only two have been characterized so far, both with stoichiometries that are common among the alkali-metal tetrelides (Tt = Si, Ge, Sn, Pb). These are KSn[3] with the NaPb-type structure[4] and K_8Sn_{46} with the K_8Si_{46}-type structure.[5] Only the analogous RbSn has been reported in the Rb−Sn system.[3] The 1:1 compounds contain isolated tetrahedral anions Sn_4^{4-}, isoelectronic with Sb_4, and are classic Zintl (valence) compounds. According to X-ray film studies in the 1960s, the K_8Tt_{46} members, Tt = Si, Ge, Sn,[5] as well as Na_8Si_{46}[6] are essentially isotypic with the $X_8(H_2O)_{46}$ clathrate-I structure[7] (X = Cl_2, SO_2, Xe, and so forth). However, there is some difficulty with this assignment as the classical Tt_{46} network is already fully four-bonded with no obvious sites for additional electrons from the alkali metals while the presumed "K_8Ge_{46}" has been reported to be a semiconductor.[9] Furthermore, the distances reported in, for example, K_8Sn_{46} remain unreasonably short (2.78−2.84 Å[3]) for a phase that presumably has eight extra electrons in antibonding states in a conduction band. The concept of vacancies in the anion lattice so as to afford a Zintl phase $K_8Ge_{44}\square_2$ instead has been raised,[10] and some direct but unpublished verifications of A_8Tt_{44} compositions and structures have been achieved.[11,12] A variety of substituted isoelectronic derivatives of the Ge_{44}^{8-} lattice have also been synthesized and characterized in support the general stability of this array.[13−15]

The present article reports a new dodecahedral cage structure for K_8Sn_{25} as well as the refinement of particularly the site occupancies for two A_8Sn_{44} phases with the nominal clathrate structure.

Experimental Section

The synthetic procedures and methods of characterization employed were similar to those for the binary rare-earth-metal gallides.[16] All materials were handled inside N_2- or He-filled gloveboxes that had typical moisture levels of less than 0.1 ppm (vol). The tin, potassium, and rubidium were cleaned with a scalpel before use. Mixtures of the elements (K, J. T. Baker, lump under oil, 98 + %; Rb, Alfa, 99.9%, sealed under Ar; Cs, Alfa, 99.98%, sealed under Ar; Sn, Baker's Analyzed 99.999%) with various nominal compositions were welded within Ta containers which were in turn sealed in fused silica jackets. The contents were melted at 1000 °C and then slowly cooled and annealed at several different temperatures. The products had dark gray appearances and were very brittle.

The K−Sn reaction conditions, product distributions estimated on the basis of powder pattern intensities, and cell parameters (Guinier) for the $K_{8\pm}Sn_{25}$ phases are given in Table 1. It will be noted that the measured lattice dimensions depend on annealing conditions as well as on composition. A phase "KSn_4" was originally proposed in this region, with an apparent phase transition near 414 °C and an incongruent melting point of 600 °C.[2] Only thermal analysis was employed. The KSn_4 composition lies almost midway between K_8Sn_{25} and K_8Sn_{44} (below), and it seems likely that the two thermal effects should be assigned to the incongruent melting of K_8Sn_{44} and K_8Sn_{25}, respectively.

[⊗] Abstract published in *Advance ACS Abstracts,* November 15, 1994.
(1) The Ames Laboratory is operated for the U.S. Department of Energy by Iowa State University under Contract No. W-7405-Eng-82. This research was supported by the Office of the Basic Energy Sciences, Materials Sciences Division, DOE.
(2) *Binary Alloy Phase Diagrams,* 2nd ed.; Massalski, T. B., Ed.; ASM International: Materials Park, OH, 1990; Vol. 3, p 2388.
(3) Hewaidy, I. F.; Busmann, E.; Klemm, W. *Z. Anorg. Allg. Chem.* **1964,** *328,* 283.
(4) Marsh, R. E.; Shoemaker, D. P. *Acta Crystallogr.* **1953,** *6,* 197.
(5) Gallmeier, J.; Schäfer, H.; Weiss, A. *Z. Naturforsch.* **1967,** *22B,* 1080; **1969,** *24B,* 665.
(6) Kaspar, J. S.; Hagenmuller, P.; Ponchard, R. M.; Cros, C. *Science* **1965,** *150,* 1713.
(7) Pauling, L.; Marsh, R. E. *Proc. Nat. Acad. Sci. U.S.A.* **1952,** *38,* 112.
(8) von Schnering, H.-G. *Angew. Chem., Int. Ed. Engl.* **1981,** *20,* 33.
(9) Cros, C.; Pouchard, M.; Hagenmuller, P.; Kasper, J. S. *Bull. Soc. Chim. Fr.* **1968,** 2737.
(10) von Schnering, H.-G. *Nova Acta Leopoldina* **1985,** *59,* 168.
(11) von Schnering, H.-G., private communication, 1994.
(12) Llanos, J. Doctoral Dissertation, University of Stuttgart, 1983.
(13) Menke, H.; von Schnering, H.-G. *Z. Anorg. Allg. Chem.* **1973,** *395,* 223.
(14) von Schnering, H.-G.; Menke, H. *Z. Anorg. Allg. Chem.* **1976,** *424,* 108.
(15) Nesper, R.; Curda, J.; von Schnering, H.-G. *Angew. Chem.* **1986,** *98,* 369.
(16) Zhao, J.-T.; Corbett, J. D. *J. Alloys Comp.* **1994,** *210,* 1.

0020-1669/94/1333-5721$04.50/0

Table 1. Products from Different K−Sn Reactions and Cell Parameters for the $K_{8\pm}Sn_{25}$ Phase

composition	cond[a]	products[b] (%)	a (Å)	V (Å^3)
$K_{12.5}Sn_{25}$	a	70 I, 30 II	16.461(3)	4461(2)
$K_{10.0}Sn_{25}$	b	80 I, 20 II	16.454(6)	4455(5)
$K_{8.5}Sn_{25}$	b	100 I	16.443(2)	4446(2)
$K_{8.0}Sn_{25}$	b	100 I	16.392(8)	4404(6)
$K_{8.0}Sn_{25}$	a	100 I	16.228(4)	4273(4)
$K_{7.8}Sn_{25}$	b	100 I	16.414(3)	4423(2)
$K_{7.5}Sn_{25}$	b	100 I	16.408(1)	4417(1)
$K_{7.5}Sn_{25}$[c]	a	>95 I	16.294(5)	4326(4)
$K_{6.25}Sn_{25}$	a	65 I, 35 III	16.278(3)	4325(5)
$K_{4.35}Sn_{25}$	a	5 I, 95 III	−	−

[a] All were heated slowly to 1000 °C, held 12 h, cooled at 2 deg h^{-1} to 850 °C, held 48 h; cooled 5 deg h^{-1} to 550 °C, held 48 h, cooled 5 deg h^{-1} to 380 °C. Then (a) annealed at 380 °C for 24 h and 360 °C for 360 h, cooled slowly to 100 °C, held 40 d, cooled to room temperature; (b) annealed at 380 °C for 120 h and cooled to room temperature. [b] I, $K_{8\pm}Sn_{25}$; II, unidentified phase; III, K_8Sn_{44}. The detection limits by Guinier diffraction are ~2−4%. [c] Data crystal reaction.

Crystals of Rb_8Sn_{44} were secured during an exploration for the nonexistent Rb_8Sn_{25}, while $K_{1.6}Cs_{6.4}Sn_{44}$ crystals were obtained from a $K_{1.5}Cs_3Sn_{25}$ composition (under conditions *a*, Table 1) in an unsuccessful attempt to occupy the different-sized cage cavities in A_8Sn_{25} with distinguishing cations. The product was mixed with ~40% A_8Sn_{25}, the powder pattern of which suggested very little substitution of cesium for potassium had occurred. Compositions were established by crystallographic refinements.

Magnetic susceptibilities and resistivities of the ideal compositions K_8Sn_{25} and K_8Sn_{44} were measured with SQUID (MPMS) and Q techniques,[17] respectively.

For the K_8Sn_{25} structural study, black crystalline chunks mounted in thin-walled glass capillaries were first checked by Laue photographs. Diffraction data from one specimen were collected at room temperature with the aid of an Enraf-Nonius CAD4 diffractometer. The routine indexing and cell reduction clearly gave a primitive cubic cell. The 4352 reflections measured without condition in the *hkl* octant up to $2\theta = 50°$ led, after an absorption correction based on the average of three ψ-scans, to 1324 unique reflections ($R_{av} = 0.106$) of which 833 were observed ($I/\sigma(I) > 3$). Systematic absences indicated only two possible, enantiomorphic space groups: $P4_132$ and $P4_332$. The structure of the crystal was solved by direct methods and refined in the former group with the program package TEXSAN.[18] Anomalous dispersion was taken into account during the refinements. Because of the well-known inadequacy of the semiempirical ψ-scan method to correct F_o data from strong absorbers at higher θ values (larger μ), a subsequent correction starting with the refined isotropic parameters was applied with DIFABS.[19] The final refinement confirmed a new structure type in the uncommon space group $P4_132$ with the composition $K_{7.4(1)}Sn_{25}$. The certainty of the cation content is limited by the anisotropic distribution within the fractionally occupied K3 site. Such refined occupancies customarily do not depend significantly on the choice of an absorption correction method.

The clathrate-like structures of the nominal Rb_8Sn_{46} and $K_xCs_{8-x}Sn_{46}$ were both similarly refined in order to confirm the structure and stoichiometry of the former, which was previously unknown, and to see whether the different sizes of the two cages in the anion lattice would distinguish mixed cations well. The data collections for one octant ($2\theta < 50°$) for each on Rigaku AFC6R and CAD4 instruments, respectively, were shortened somewhat through the use of shorter scan times and higher cutoffs for the weaker reflections. The refinements were entirely routine; absorption was handled as before. Only the occupancies of the 6*c* (Sn3) positions deviated significantly from unity. The mixed K + Cs positions were refined as fully occupied, as they are with Rb. Some details of the three structural studies are given in Table 2, while positional and isotropic-equivalent displacement parameters for the atoms appear in Tables 3 and 4. The anisotropic displacement parameters are in supplementary material and are also available from J.D.C. along with the structure factor data.

Table 2. Selected Details of the Structural Studies

composition	$K_{7.4(1)}Sn_{25}$	$Rb_8Sn_{44.6(1)}$	$K_{1.6(2)}Cs_{6.4(2)}Sn_{44.0(1)}$
space group, Z	$P4_132$ (no. 213), 4	$Pm\bar{3}n$ (no. 223), 1	$Pm\bar{3}n$ (no. 223), 1
cell parameters: a (Å)[a]	16.294(5)	12.054(1)	12.084(1)
V (Å^3)	4326(4)	1751(3)	1765(4)
fw; d_{calc} (g cm^{-3})	4326; 4.999	5978; 5.667	6136; 5.773
μ (Mo Kα) (cm^{-1})	149.2	210.3	186.5
transm range	0.91−1.05	0.63−1.15	0.61−1.42
residuals: R_w[b]/R[c] (%)	3.6/4.0	6.7/7.6	5.7/6.6

[a] From Guinier powder data with Si as internal standard; λ = 1.540 562 Å, 22 °C. [b] $R_w = [\sum w(|F_o| - |F_c|)^2/\sum w(F_o)^2]^{1/2}$, $w = \sigma_F^{-2}$. [c] $R = \sum||F_o| - |F_c||/\sum|F_o|$.

Table 3. Atom Positional and Isotropic Displacement Parameters for $K_{7.4(1)}Sn_{25}$

atom	site	x	y	z	B_{eq}[a] Å^2
Sn1	8*c*	0.0324(1)	x	x	1.4660(7)
Sn2	24*e*	0.2037(1)	0.0442(1)	0.0007(1)	1.27(7)
Sn3	12*d*	1/8	0.1669(1)	1/4 + x	1.56(6)
Sn4	24*e*	0.2397(1)	0.9342(1)	0.8723(1)	1.36(7)
Sn5	24*e*	0.4173(1)	0.8512(1)	0.0864(1)	1.92(8)
Sn6	8*c*	0.3246(1)	x	x	1.8368(7)
K1	8*c*	0.1903(4)	x	x	3.042(3)
K2	4*b*	7/8	7/8	7/8	15.93(2)
K3[b]	24*e*	0.6885(8)	0.9590(9)	0.537(1)	13(1)

[a] $B_{eq} = (8\pi^2/3)\sum_i\sum_j U_{ij}a_i^*a_j^*\vec{a}_i\vec{a}_j$. [b] Occupancy = 0.73(2).

Table 4. Atom Positional and Isotropic Displacement Parameters for A_8Sn_{44} Phases

atom	site	x	y	z	occup	B_{eq}[a] (Å^2)
			$Rb_8Sn_{44.6(1)}$			
Sn1	24*k* (*m*)	0	0.3180(3)	0.1189(3)	1	3.3 (2)
Sn2	16*i* (3)	0.1828 (2)	x	x	1	1.847 (1)
Sn3	6*c* ($\bar{4}2m$)	1/4	0	1/2	0.77(2)	1.8 (2)
Rb1	2*a* ($m\bar{3}$)	0	0	0	1	1.821 (3)
Rb2	6*d* ($\bar{4}m2$)	1/4	1/2	0	1	3.9 (3)
			$K_{1.6(2)}Cs_{6.4(2)}Sn_{44.0(1)}$			
Sn1		0	0.3164 (3)	0.1192 (3)	1	3.29 (1)
Sn2		0.1829 (1)	x	x	1	1.642 (1)
Sn3		1/4	0	1/2	0.67(1)	1.1 (2)
A1		0	0	0	1.0[b]	1.124 (5)
A2		1/4	1/2	0	1.0[c]	2.7 (1)

[a] $B_{eq} = (8\pi^2/3)\sum_i\sum_j U_{ij}a_i^*a_j^*\vec{a}_i\vec{a}_j$. [b] A1 = $K_{0.67(4)}Cs_{0.33(4)}$. [c] A2 = $K_{0.04(2)}Cs_{0.96(2)}$.

Results and Discussion

K_8Sn_{25}. The structure refined for $K_{7.4}Sn_{25}$ is evidently the first among intermetallic compounds that is constructed from pentagonal dodecahedra, that is, M_{20} units. The tin anion network is built up mainly by sharing three of 12 pentagonal faces of each Sn_{20} unit with other like polyhedra. The Sn_{20} figure in this compound is deformed from the ideal I_h point group to C_3, although it deviates only slightly from a C_{3v} symmetry. Its illustration in Figure 1 includes all adjoining Sn atoms that are bonded to members of this cage, mainly through sharing of the shaded faces. The cluster is centered by K1, and a 3-fold axis through Sn1−K1−Sn6 lies about normal to the page. This Sn1 as well as three Sn5 atoms adjoining Sn6 in the cage are only three-bonded, each being common to three

(17) Shinar, J.; Dehner, B.; Beaudry, B. J.; Peterson, D. T. *Phys. Rev.* **1988**, *B37*, 2066.
(18) TEXSAN, version 6.0; Molecular Structure Corp.: The Woodlands, TX, 1990.
(19) Walker, N.; Stuart, D. *Acta Crystallogr.* **1983**, *A39*, 158.

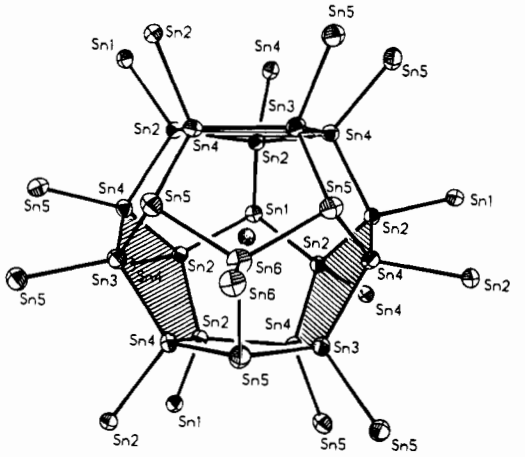

Figure 1. The dodecahedral building block in K_8Sn_{25}. The exo tin atoms are members of like polyhedra that share three faces (shaded) or the single Sn6–Sn6 bond. A 3-fold axis nearly normal to the page runs through Sn1–K1(center)–Sn6. Note that Sn1 and the three Sn5 atoms are only three-bonded (50% probability ellipsoids.)

pentagons that are unshared with neighboring polyhedra. (The Sn3 atoms also lie on 2-fold axes that bisect the Sn5–Sn3–Sn5 and Sn4–Sn3–Sn4 angles.) The Sn–Sn separations, Table 5, range from 2.816 to 2.861 Å, with only marginal differences between three- and four-bonded atoms. The Sn–Sn distances average 2.84 Å, only slightly larger than the 2.810 Å bond length in the diamond form of tin but distinctly (and appropriately) much less than the 3.02 (×4) Å and 3.18 Å (×2) Å distances in metallic Sn. Bond lengths in anionic tin arrays generally increase with effective charge, presumably from coulombic effects, as well as with the number of like neighbors and, of course, strain. Distances in the lowest charged lattice in A_8Sn_{44} phases with Rb^+ and K^+ plus Cs^+ cations (below) average a very comparable 2.82 Å. The $\bar{d}$(Sn–Sn) values increase to 2.94 Å in Sn_5^{2-} (D_{3h})[20] and 2.94–3.08 Å in Sn_9^{3-},[21] both of which occur in compounds with large cations, and to 2.97 Å in Sn_4^{4-} (T_d) in β-NaSn[22] and 2.94 Å in the two-bonded Sn chains in SrSn.[23]

The principal deformations within the dodecahedra arise because Sn1 and the three Sn5 atoms are each three-bonded, while the remainder are bonded to four tins. This makes the former four protrude somewhat from the best sphere for the cage and exhibit smaller vertex angles, 97.1–101.5° (less s hybridization). Conversely, all angles >110.0° are associated with an adjoining central atom bonded to Sn1 or Sn5. The remaining angles average 106.2°. The combination of three Sn5 atoms bonded to a central Sn6, several cation neighbors about each Sn5 (below), and, presumably, the exo Sn6–Sn6 bond put the Sn6 atom only 0.68 Å outside of the 3Sn5 plane. The result is a dodecahedron that is somewhat compressed on the Sn6 side and stretched at the opposite Sn1 vertex, as will be evident in a later figure. Thus d(Sn6–K1) is only 3.79 Å, which probably limits the adjoining Sn5–K1 to 4.46 Å, while the opposed Sn1–K1 separation is 4.17 Å. The 15 other four-bonded tin atoms are 3.77–4.01 Å from K1. For comparison, the K–Sn distances in "K_8Sn_{46}" within the pentagonal dodecahedra are about 3.81 (×8) and 3.99 (×12) Å.[5]

Figure 2 shows how the tin dodecahedra form a helical chain along each 4_1 axis by sharing pairs of faces (shaded). The full network structure is obtained by extending these chains along the other two dimensions through both the sharing of a third pentagonal face and joining these with the Sn6–Sn6 links. A portion of this condensation plus other features are shown in Figure 3, a central cage nested in three shared clusters. Its 3-fold axis along Sn1 and the Sn6–Sn6 exo link to another cluster (which is somewhat tilted toward the viewer) also contains a K2 atom beyond Sn1. The arrangement around K2 is replicated by a 2-fold axis perpendicular to the 3-fold axis, and the same operation applies at the midpoint of the Sn6–Sn6 bond.

The K2 and K3 ions in K_8Sn_{25} lie in channels through the tin network. Since three-bonded tin bears a formal −1 charge (and, more certainly, a −1 oxidation state), one would expect Sn5 and Sn1 to be preferred neighbors for potassium ions. In fact, K2 has six Sn5 neighbors at 3.80 Å in a nearly regular octahedron (D_3 rigorously), as shown in Figure 4. The large ellipsoid for K2 (15.9 Å^2) possibly arises because of its relatively low coordination number ($r_{K^+}/r_{Sn^-} = 0.67$ based on crystal radii) and, perhaps, because there are also three fractionally occupied K3 sites 3.91 Å away. On the other hand, the Sn1 vertex is relatively protected by the K2(Sn5)$_6$ unit from neighboring polyhedra (Figure 3) and has only relatively distant interactions with potassium.

Table 5. Interatomic Distances (Å) and Angles (deg) in $K_{7.4}Sn_{25}$

Sn1–3Sn2	2.845(2)	K1–3Sn4	3.770(4)
3K3	3.62(1)	Sn6	3.79(1)
K2	4.442(3)	3Sn3	3.862(4)
K1	4.46(1)	3Sn2	3.906(9)
Sn2–Sn4	2.816(3)	3Sn2	3.987(5)
Sn4	2.839(3)	3Sn4	4.011(4)
Sn1	2.845(2)	3Sn5	4.166(9)
Sn2	2.846(3)	Sn1	4.46(1)
K1	3.906(9)	K2–6Sn5	3.801(2)
K1	3.987(5)	6K3	3.91(2)
K3	4.07(1)	2Sn1	4.442(3)
K3	4.25(1)	K3–K3	2.92(4)
Sn3–2Sn4	2.846(2)	Sn5	3.49(2)
2Sn5	2.861(3)	Sn5	3.51(1)
2K3	3.60(1)	Sn3	3.60(1)
2K1	3.862(4)	Sn1	3.60(1)
Sn4–Sn2	2.816(3)	Sn4	3.77(1)
Sn2	2.839(3)	Sn5	3.89(1)
Sn3	2.846(2)	Sn4	3.89(1)
Sn5	2.859(3)	K2	3.91(2)
K1	3.770(4)	Sn2	4.07(1)
K3	3.77(1)	Sn5	4.16(1)
K3	3.89(1)	Sn2	4.25(1)
K1	4.011(4)	Sn6	4.34(1)
Sn5–Sn6	2.841(2)		
Sn4	2.859(3)		
Sn3	2.861(3)		
K3	3.49(2)		
K3	3.51(1)		
K2	3.801(2)		
K3	3.89(2)		
K3	4.16(1)		
K1	4.166(9)		
Sn6–3Sn5	2.841(2)		
Sn6	2.844(6)		
K1	3.79(1)		
3K3	4.34(1)		
Sn2–Sn1–Sn2	97.11(9)	Sn2–Sn4–Sn2	100.02(6)
Sn4–Sn2–Sn4	100.57(6)	Sn2–Sn4–Sn3	109.91(7)
Sn4–Sn2–Sn1	107.22(8)	Sn2–Sn4–Sn5	110.83(8)
Sn4–Sn2–Sn2	109.46(8)	Sn2–Sn4–Sn3	107.97(8)
Sn4–Sn2–Sn1	118.90(7)	Sn2–Sn4–Sn5	118.44(7)
Sn4–Sn2–Sn2	107.71(5)	Sn3–Sn4–Sn5	109.21(7)
Sn1–Sn2–Sn2	112.05(8)	Sn6–Sn5–Sn4	101.50(7)
Sn4–Sn3–Sn4	107.7(1)	Sn6–Sn5–Sn3	101.30(7)
Sn4–Sn3–Sn5	110.23(5)	Sn4–Sn5–Sn3	98.03(7)
Sn4–Sn3–Sn5	111.92(5)	Sn5–Sn6–Sn5	114.61(5)
Sn5–Sn3–Sn5	104.9(1)	Sn5–Sn6–Sn6	103.65(7)

(20) Edwards, R. A.; Corbett, J. D. *Inorg. Chem.* **1977**, *16*, 903.
(21) Critchlow, S. C.; Corbett, J. D. *J. Am. Chem. Soc.* **1983**, *105*, 5715.
(22) Müller, W.; Volk, K. *Naturforsch.* **1977**, *32B*. 709.
(23) Widera, A.; Schäfer, H. *J. Less-Common Met.* **1981**, *77*, 29.

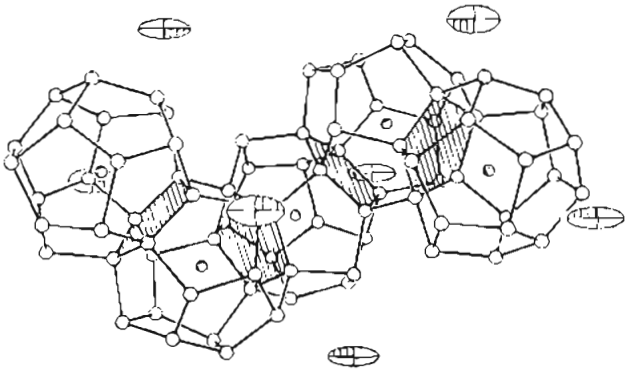

Figure 2. Part of a helical chain in K_8Sn_{25} formed by sharing two faces of each cage, along with adjoining K3 ions in the tunnels.

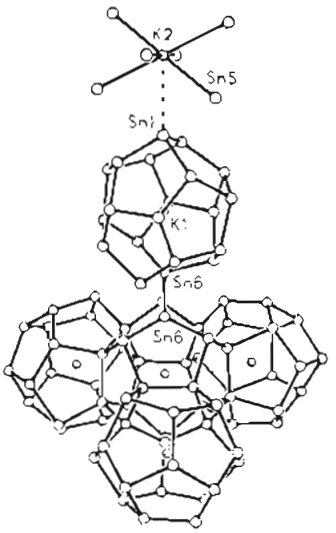

Figure 3. The nesting of four Sn_{20} cages, the exo Sn6−Sn6 bond between the central unit and another cluster, and the $K2(Sn5)_6$ unit along the 3-fold axis in K_8Sn_{25} (arbitrary spheres). (Horizontal 2-fold axes also pass through the K2 atoms and the midpoints of the Sn6−Sn6 bonds.)

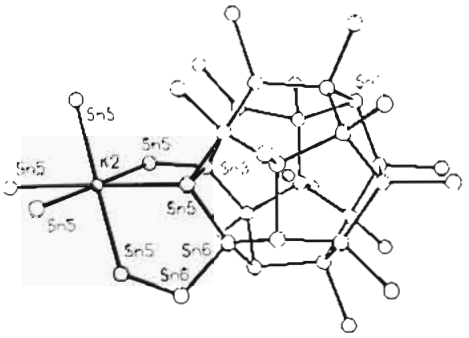

Figure 4. The K2 environment adjoining an Sn_{20} cage in K_8Sn_{25}.

Figure 5 is perspective views of the whole structure along (a) the 4_1- (cell-) axis and (b) the 3-fold [111] axis to emphasize the nature and magnitudes of the channels. All of the K1@Sn_{20} dodecahedra cages in these views have been replaced by spheres, and their line interconnections represent the three shared faces. The K2 and K3 atoms, striped and open circles, respectively, are distributed in a 1:6 ratio within the network channels.

The K3 sites, which show a 73% occupancy for the refined composition $K_{7.4(1)}Sn_{25}$ (and 83.3% at the ideal K_8Sn_{25}), require special note. These atoms are less well defined positionally, and their B's are fairly large, 13 Å^2, with an extreme U_{ii}/U_{jj} axial ratio of ~7. This appears to result from the lack of a reasonable coordination polyhedron, as shown in Figure 6 (with

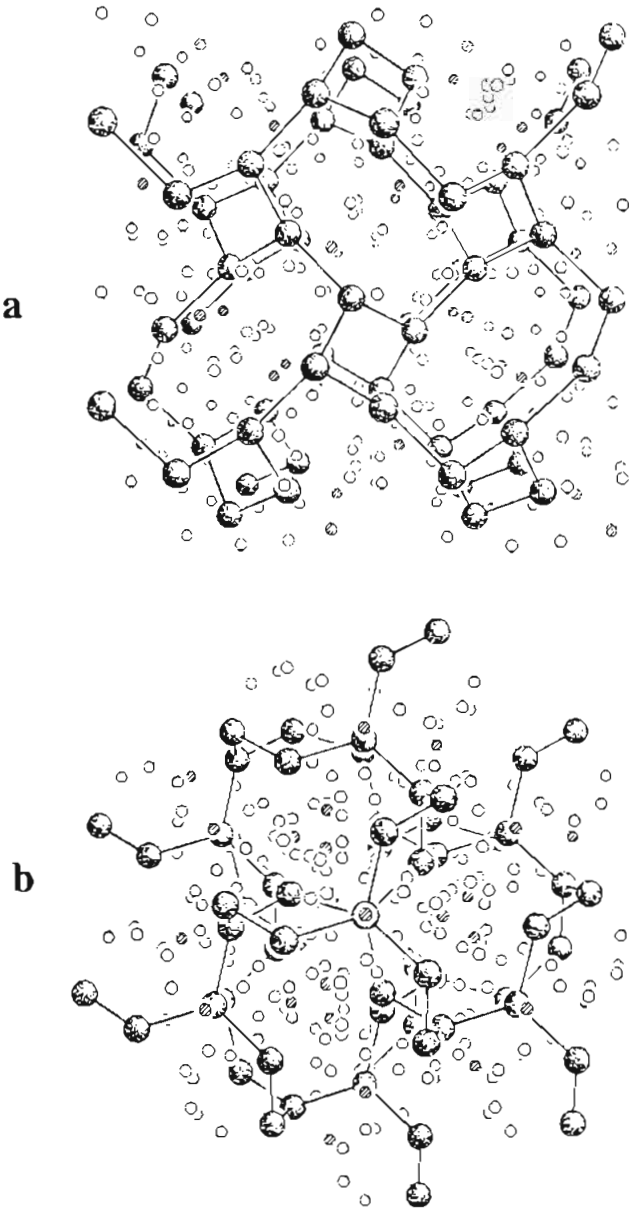

Figure 5. Perspective views of the whole K_8Sn_{25} structure (a) along [100], (b) along [111]. The tin cages are represented by spheres and their shared faces, by the interconnecting lines. The K2 and K3 atoms are striped and open circles, respectively.

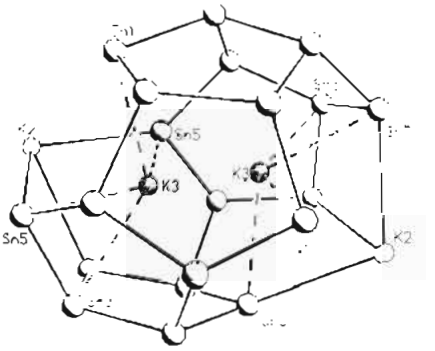

Figure 6. The K3 environment in K_8Sn_{25} with close contacts to four cage tins marked (see text).

arbitrary ellipsoids). The four tin neighbors to K3 at 3.49−3.60 Å are the shortest d(K−Sn) in the structure, and all lie on one side, while an opposed K3 neighbor is only 2.92(4) Å away. Such positional problems are characteristics of guest atoms (or molecules) in zeolitic structures. Refinement with the reduced

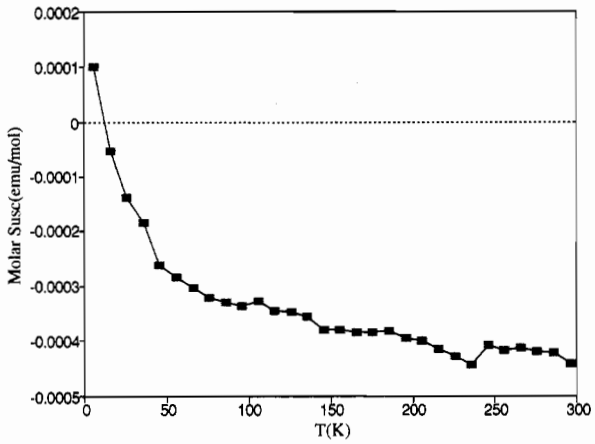

Figure 7. The molar magnetic susceptibility of K_8Sn_{25} as a function of temperature (K).

symmetry of space group $P2_13$ did not allow any further ordering of the K3 positions to be resolved.

The ideal stoichiometry for a Zintl (valence) compound with this structure would be K_8Sn_{25}, which derives from the fact that 8 of 25 tin atoms are 3b-Sn^{-1} (Sn1, Sn5) the remainder 4b-Sn^0. In more detail, this corresponds to $[(K^+)_4(4b\text{-}Sn)_{15/2}(4b\text{-}Sn6)(3b\text{-}Sn^{-1})_4]_2$. The unit cell parameters obtained for K_8Sn_{25} from different loaded stoichiometries and annealing conditions were given in Table 1. The reaction products $K_{8\pm}Sn_{25}$ at fixed stoichiometry seem to exhibit significant dependences of cell dimensions on reaction conditions, a 0.16 Å (1.0%) decrease accompanying further annealing of the ideal stoichiometry at 100 °C rather than 360 °C. (The data crystal for the diffraction study was so treated.) These differences presumably reflect (unknown) changes in cation ordering (and perhaps partially, some small inherent stoichiometry differences between samples). The unit cell parameters as a function of composition are also at or near minimum values for the ideal stoichiometry K_8Sn_{25} under both annealing conditions. The stoichiometry breadth is better defined by the samples last annealed at 360 °C, for which the range is of the order of $K_{7.8}Sn_{25}$ to $K_{8.5}Sn_{25}$. Volume increases on either side of the ideal are easy to understand. With less K, Sn−Sn bond orders are reduced (holes appear in the valence band or at the formal lone pairs on 3b-Sn^{-1}), while an excess of cations naturally expands the lattice and may also afford antibonding effects. In view of the problems reflected in Figure 6, the addition of more potassium to the substoichiometric structure that was refined may mean other sites become occupied. The use of mixed cations in A_8Sn_{25} to influence the cation ordering within the channels could prove interesting, but the phase does not form when A is pure Na or Rb, presumably reflecting a considerable sensitivity to cation size, especially within the Sn_{20} dodecahedron (K1). Both of these A_8Sn_{25} compositions contain the A_8Sn_{44} phase instead.

An isotypic compound has been independently established for $Ba_6In_4Sn_{21}$[11,24] in the same chirality. In this case, indium partially substitutes, in decreasing amounts, at the equivalent of Sn2, Sn3, and Sn6, while half of the barium occupies K1- and K2-type sites. The remaining Ba lies in a different 12-*d* site with a similarly elongated distribution.

Properties. Physical properties of the phase at the K_8Sn_{25} composition are nicely supportive of a Zintl phase formulation. The small, core-corrected magnetic susceptibility data shown in Figure 7 indicate the phase is generally diamagnetic with electrons in closed shells. The temperature dependence is reasonable for low effective masses in a semiconductor.[25] The conductivity measurements by the high-frequency Q-method showed a semiconductor-like temperature dependence, but these did not yield an accurate band gap owing to the very small ΔQ readings (high resistivities). The semiquantitative result is $E_g > 0.2$ eV with a room temperature resistivity of ~750 $\mu\Omega$·cm. This and the chiral structure may provide some very interesting nonlinear electronic properties. Furthermore, the helical channels may also afford some useful ionic conduction if the K3 cations can be substituted by a smaller ions such as Na or Li, provided the structure is retained and that the Li^+ cations especially do not strongly polarize a local electron density or site.

It is useful to put the Sn_{20} pentagonal dodecahedron in perspective. The pentagonal dodecahedron is one of the regular (Platonic) polyhedra and, with 20 vertices, it is the conjugate form (face-vertex dual) of the much more common icosahedron. This dodecahedron is also the geometric limit of the fullerene family. According to Euler's theorem, three-bonded polyhedra consisting entirely of hexagons and pentagons have no restrictions as to the number of hexagons on the surface (other than with only one[26]), while the number of pentagons required is exactly 12.[27] (Of course, there is no assurance that examples of all of these will exist.) The pentagonal dodecahedron is the limit with no hexagons in the polyhedron. The 14-face polyhedron found in the A_8Tr_{44} structure (below) has two hexagons, the 16-face polyhedron in the $A_{24}(H_2O)_{136}$ clathrate-II structure[28,29] is that with four hexagons, the C_{60} fullerene has 20 hexagons, and the In_{74} cage in $Na_{96}In_{97}Ni_2$ has 27.[30] Although small fullerene molecules such as C_{44} with 12 hexagons exist, a still smaller dodecahedral C_{20} is not expected to be stable owing to the severe strain and an open shell in the π-bonding.[31] The recent association of the gaseous Ti_8C_{12}[32] cluster with a sort of pentagonal dodecahedron suggests a molecule that is very stable in terms of both spherical geometry and a bonding structure.

A_8Sn_{44}. The structures of two examples of the supposed clathrate-I structure were refined in order to clarify both the electron count of the anion network and the Sn−Sn bond distances relative to other examples, K_8Sn_{25} in particular. The closest portion of familiar clathrate cell contents are shown in projection in Figure 8. Nonintersecting chains of 14-faced tin polyhedra that share hexagonal faces lie across the centers of all cube faces, and these polyhedra are all centered by A2 cations (larger spheres, $\bar{4}m2$ or D_{2d} point symmetry). (The horizontal chains that lie in the top and bottom faces of the cell are not shown in this view.) The collection of such chains define pentagonal-faced dodecahedra about the cell origins, and these are centered by A1 cations (point symmetry $m\bar{3}$ or D_{3d}; the 3-fold axes lie in the cube diagonals). The essence of the A_8Sn_{44} stoichiometry variation that affords a Zintl phase (closed shell) behavior is that one-third of the Sn3 (6*c*) positions (shaded ellipsoids) which lie across the shared hexagons are left empty (randomly). This particular atom type is a member of only this array of chains and has all neighbors the same (Table 6). The eight Sn1 neighbors per cell around these vacancies are thus

(24) Kröner, R. Doctoral Dissertation, University of Stuttgart, 1989.

(25) Martin, D. H. *Magnetism in Solids*; The MIT Press: Cambridge, MA, 1967; p 179.
(26) Gruenbaum, B.; Motzkin, T. S. *Can. J. Math.* **1963**, *347*, 744.
(27) Chung, F.; Sternberg, S. *Am. Sci.* **1993**, *81*, 56.
(28) Gros, C.; Pouchard, M.; Hagenmuller, P. *Bull. Soc. Chim. Fr.* **1963**, *2*, 379.
(29) Gros, C.; Benejat, J.-C. *Bull. Soc. Chim. Fr.* **1971**, *5*, 1739.
(30) Sevov, S. C.; Corbett, J. D. *Science* **1983**, *262*, 880.
(31) Kroto, H. W. *Nature* **1987**, *329*, 530.
(32) Guo, B. C.; Kerns, K. P.; Castleman, A. W., Jr. *Science* **1992**, *255*, 1411.

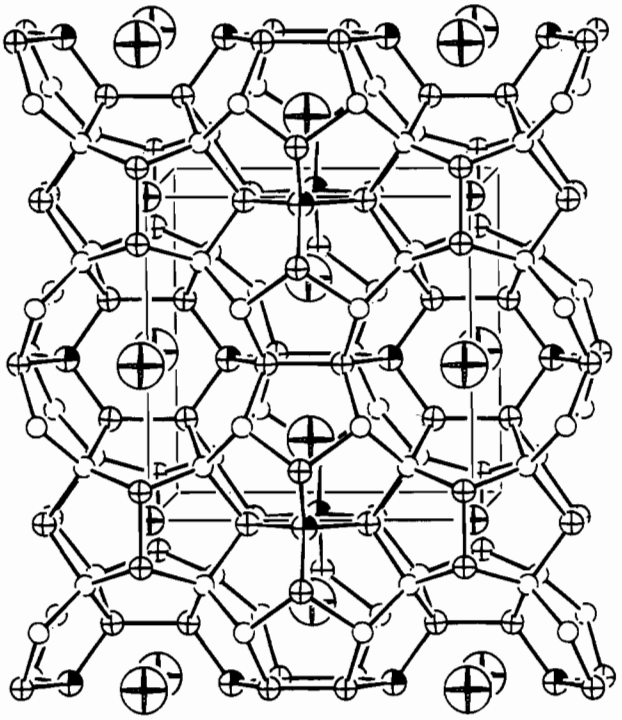

Figure 8. A portion of the cubic A_8Sn_{44} structure with large crossed spheres denoting both A1 atoms within dodecahedra at cell corners and A2 atoms that center 14-faced polyhedra along $^1/_2,0,(^1/_4,^3/_4)$, etc. Tin atoms are interconnected and keyed as Sn1 (crossed), Sn2 (open), Sn3 (shaded) (67% occupied).

Table 6. Distances (Å) in Two A_8Sn_{44} Structures

	Rb_8Sn_{44}	$K_{1.6}Cs_{6.4}Sn_{44}$
Sn1−Sn1	2.868 (8)	2.881 (6)
Sn1−2Sn2	2.847 (3)	2.843 (2)
Sn1−Sn3	2.703 (4)	2.724 (4)
Sn2−3Sn1	2.847 (3)	2.843 (2)
Sn2−Sn2	2.807 (7)	2.811 (5)
Sn3−4Sn1	2.703 (4)	2.724(4)
Sn1−A1	4.093 (4)	4.086 (4)
Sn1−2A2	3.993 (2)	4.015 (2)
Sn2−A1	3.816 (4)	3.827 (3)
Sn2−3A2	4.487 (1)	4.4977 (9)
Sn3−4A2	4.2616 (3)	4.2725 (3)
A1[a]−12Sn1	4.093 (4)	4.086 (4)
A1[a]−8Sn2	3.816 (4)	3.827 (3)
A2−12Sn1	3.993 (2)	4.015 (2)
A2−8Sn2	4.487 (1)	4.4977 (9)
A2−4Sn3	4.2616 (3)	4.2725 (3)

[a] In dodecahedron.

3b-Sn^{-1}, giving $(K^+)_8(3b\text{-}Sn^{-1})_8(4b\text{-}Sn^0)_{36}$. A sample with a K_8Sn_{44} stoichiometry was found to be a diamagnetic semiconductor with $E_g \sim 0.25$ eV and $\varrho_{293} \approx 288$ $\mu\Omega$·cm.

The different sizes of the two types of polyhedra in this structure and the probable existence of a matrix effect in the smaller cavity are reflected in the 0.18 Å difference in nearest neighbor Rb−Sn distances between the two, about 50% greater than given by Shannon[33] for the CN8 → CN12 change. The better accommodation of mixed cations in the $K_{1.6}Cs_{6.4}Sn_{44}$ phase (synthesized from a Cs-rich) melt) means the smaller A1 site is about two-thirds occupied by K (with a marginal increase in d(Al−Sn) relative to Rb_8Sn_{44}) while the A2 position is occupied by nearly pure cesium, which enlarges that cavity by twice as much (0.022 Å, 7.8 σ). There are no overall changes of statistical significance in average Sn−Sn distances between the two phases, however (Table 6).

The presence of such electronically poor tetrelide networks in Zintl phases with this structure type via either defects (as above) or substitution of electron-poorer elements has been established in several (unpublished) instances by von Schnering and co-workers.[11] Structures of the binary phases have been refined for $K_8Ge_{44.3}$[12] and $Cs_8Sn_{44.0}$.[24] Isostructural, semiconducting line phases of the type $A_8Tr_6Tt_{40}$ have been synthesized and their structures refined for a wide variety of combinations: A = K−Cs; Tr = Al, Ga, In; Tt = Si, Ge, Sn. In each case about eight Tr elements per cell substitute on all three Tt sites in the general order $6c > 24k > 16i$, Tr being the major components in the first position.[24]

The general A_8Y_{46} lattice shown in Figure 8 will also be recognized as a scaled A15 (V_3Si-type) structure in which the 14-face polyhedral chains replace the chains of vanadium while the dodecahedra replace the silicon atoms. A face-vertex dual analogy is nearly achieved between the ideal A_8Y_{46} and the recently described A15-like $A_3Na_{26}In_{48}$ (A = K, Rb, Cs) in which hexagonal antiprismatic In_{12} units, *arachno*-In_{14} that is, are interbonded with one-third as many In_{12} icosahedra in the same lattice.[34,35] Only the two missing vertices in the former cage spoil an exact relationship. In the indium case, all cluster members are appropriately connected by intercluster bonds between vertices rather than via face sharing. The diverse instances in which efficient, space-filling, bonding arrangements repeat is both surprising and pleasing.

Acknowledgment. The authors are indebted to J. Ostenson for the magnetic data, J. Shinar for the Q-meter use, and M. Köckerling for help with the drawings. H.-G. von Schnering generously provided information on related unpublished research.

Supplementary Material Available: Details of data collection and refinement and anisotropic displacement parameters for the three structures (Tables S1-S4) (3 pages). Ordering information is given on any current masthead page.

(33) Shannon, R. D. *Acta Crystallogr.* **1976**, *32A*, 752.
(34) Sevov, S. C.; Corbett, J. D. *Inorg. Chem.* **1993**, *32*, 1612.
(35) Carrillo-Cabrera, W.; Caroca-Canaks, N.; Peters, K.; von Schnering, H.-G. *Z. Anorg. Allg. Chem.* **1993**, *619*, 1556.